Wang S, Qiu L, Yan X, Jin W, Wang Y, Chen L et al (2012) Loss of microRNA 122 expression in patients with hepatitis B enhances hepatitis B virus replication through cyclin G(1)-modulated P53 activity. Hepatology 55(3):730–741

Wasley A, Alter MJ (2000) Epidemiology of hepatitis C: geographic differences and temporal trends. Semin Liver Dis 20(1):1–16

Wong DK, Yuen MF, Poon RT, Yuen JC, Fung J, Lai CL (2006) Quantification of hepatitis B virus covalently closed circular DNA in patients with hepatocellular carcinoma. J Hepatol 45(4):553–559

Wu X, Wu S, Tong L, Luan T, Lin L, Lu S et al (2009) miR-122 affects the viability and apoptosis of hepatocellular carcinoma cells. Scand. J Gastroenterol 44(11):1332–1339

Xia T, O'Hara A, Araujo I, Barreto J, Carvalho E, Sapucaia JB et al (2008) EBV microRNAs in primary lymphomas and targeting of CXCL-11 by ebv-mir-BHRF1-3. Cancer Res 68(5):1436–1442

Xie X, Piao L, Bullock BN, Smith A, Su T, Zhang M et al (2013) Targeting HPV16 E6-p300 interaction reactivates p53 and inhibits the tumorigenicity of HPV-positive head and neck squamous cell carcinoma. Oncogene. doi:10.1038/onc.2013.25. [Epub ahead of print]

Xu N, Papagiannakopoulos T, Pan G, Thomson JA, Kosik KS (2009) MicroRNA-145 regulates OCT4, SOX2, and KLF4 and represses pluripotency in human embryonic stem cells. Cell 137(4):647–658

Yan H, Zhong G, Xu G, He W, Jing Z, Gao Z et al (2012) Sodium taurocholate cotransporting polypeptide is a functional receptor for human hepatitis B and D virus. eLife 1:e00049

Yi R, Poy MN, Stoffel M, Fuchs E (2008) A skin microRNA promotes differentiation by repressing 'stemness'. Nature 452(7184):225–229

Yu F, Yao H, Zhu P, Zhang X, Pan Q, Gong C et al (2007) let-7 regulates self renewal and tumorigenicity of breast cancer cells. Cell 131(6):1109–1123

Zhang GL, Li YX, Zheng SQ, Liu M, Li X, Tang H (2010) Suppression of hepatitis B virus replication by microRNA-199a-3p and microRNA-210. Antivir Res 88(2):169–175

Zhang X, Zhang E, Ma Z, Pei R, Jiang M, Schlaak JF et al (2011a) Modulation of hepatitis B virus replication and hepatocyte differentiation by MicroRNA-1. Hepatology 53(5):1476–1485

Zhang Y, Xie RL, Croce CM, Stein JL, Lian JB, van Wijnen AJ et al (2011b) A program of microRNAs controls osteogenic lineage progression by targeting transcription factor Runx2. Proc Natl Acad Sci U S A 108(24):9863–9868

Zheng ZM, Baker CC (2006) Papillomavirus genome structure, expression, and post-transcriptional regulation. Front Biosci 11:2286–2302

Zhou J, Yu L, Gao X, Hu J, Wang J, Dai Z et al (2011) Plasma microRNA panel to diagnose hepatitis B virus-related hepatocellular carcinoma. J Clin Oncol 29(36):4781–4788

Zhu JY, Pfuhl T, Motsch N, Barth S, Nicholls J, Grasser F et al (2009) Identification of novel Epstein-Barr virus microRNA genes from nasopharyngeal carcinomas. J Virol 83(7):3333–3341

Ziegelbauer JM, Sullivan CS, Ganem D (2009) Tandem array-based expression screens identify host mRNA targets of virus-encoded microRNAs. Nat Genet 41(1):130–134

みにれびゅう

器官サイズを調節する転写共役因子YAPの活性制御

畠　星治[1,2]，堅田　利明[1]，仁科　博史[2]

1. はじめに

組織における細胞の数の制御は，器官のサイズや組織の恒常性の維持に必須であり，この破綻は器官形成不全や発がんに至る．がん抑制シグナル伝達経路の一つであるHippo経路は，細胞の増殖，生死，分化などを制御して組織における「細胞の数」を調節し，器官のサイズや組織の恒常性を維持している[1]．YAP（yes-associated protein）とそのパラログであるTAZ（transcriptional coactivator with PDZ-binding motif）は，Hippo経路の中心的な役割を果たす転写共役因子である．YAPとTAZはさまざまな遺伝子発現の誘導を介して細胞増殖を促進し細胞死を抑制することでHippo経路のエフェクターとして機能する．近年では多様なHippo経路の上流の制御機構が明らかにされ，細胞が接触する細胞外基質や隣接する細胞との接着といった細胞の接触状態の違いによってHippo経路の活性が巧妙に制御されていることが明らかになりつつある．本稿では，Hippo経路の中心的役割を担うYAPの制御機構に焦点をあて，進展の目覚ましい本領域における最新の知見を哺乳動物に関するものを中心として概説するとともに，我々が最近明らかにした翻訳後修飾を介したYAPの新たな制御機構に関する研究成果を紹介する．

2. YAPによる器官サイズと発がんの制御

器官のサイズは，構成する「細胞の数」と「個々の細胞の大きさ」によって規定されており，Hippo-YAP経路は器官における「細胞数」の制御を担う（図1）．一方，「個々の細胞の大きさ」は栄養状態を感知するmTOR経路により制御されていることが知られているが，多くの場合，器官のサイズ制御は「細胞の数」に依存している[1]．肝臓や心臓などのいくつかの器官においてYAP依存的にサイズが制御されていることが示されており，特に肝臓においては顕著である．マウス肝臓の肝実質細胞においてYAPを過剰発現させると，肝実質細胞の増殖が亢進し，通常は全体重の約5%に維持されている肝臓重量比が約25%にまで増大することが示されている[2]．興味深いことに，肝臓が増大した後にYAPの発現誘導を中止すると，肝臓は元のサイズにまで戻る．これは，肝臓のサイズがYAP依存的に可逆的に制御されていることを示唆している．さらに，長期間にわたってYAPの発現を誘導すると，肝細胞がんの発症に至る．肝細胞がんを含むヒトのさまざまな種類のがん症例において，YAP遺伝子座を含むゲノム領域が増幅しており，YAPの発現量の増加や核内局在の亢進が報告されていることからも，YAPはがん遺伝子産物であることが明らかとなっている[3,4]．

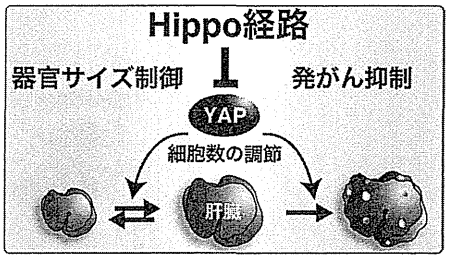

図1　Hippo-YAP経路による器官サイズ制御と発がん抑制

3. Hippo経路によるリン酸化を介したYAPの機能抑制機構

哺乳動物のHippo経路の主要構成因子はショウジョウバエのHippoのホモログであるMst1/2（mammalian ste20-like kinase 1と2），Lats1/2（large tumor suppressor 1と2），Sav（salvador），Mobl（mps one binder 1），YAPとTAZおよびTEAD1/2/3/4/である[1]（図2A）．YAPとTAZは転写共役因子であり，転写活性化ドメインを有するもののDNA結合ドメインは持たない．このため，YAPは核内にてさまざまな転写因子と結合することで各々の転写因子が標的

[1] 東京大学大学院薬学系研究科生理化学教室（〒113-0033 東京都文京区本郷7-3-1）
[2] 東京医科歯科大学難治疾患研究所発生再生生物学分野

Regulations of YAP transcriptional co-activator

Shoji Hata[1,2], Toshiaki Katada[1] and Hiroshi Nishina[2]
([1]Laboratory of Physiological Chemistry, Graduate School of Pharmaceutical Sciences, The University of Tokyo, 7-3-1 Hongo, Bukyo-ku, Tokyo 113-0033, Japan; [2]Department of Developmental and Regenerative Biology, Medical Research Institute, Tokyo Medical and Dental University)

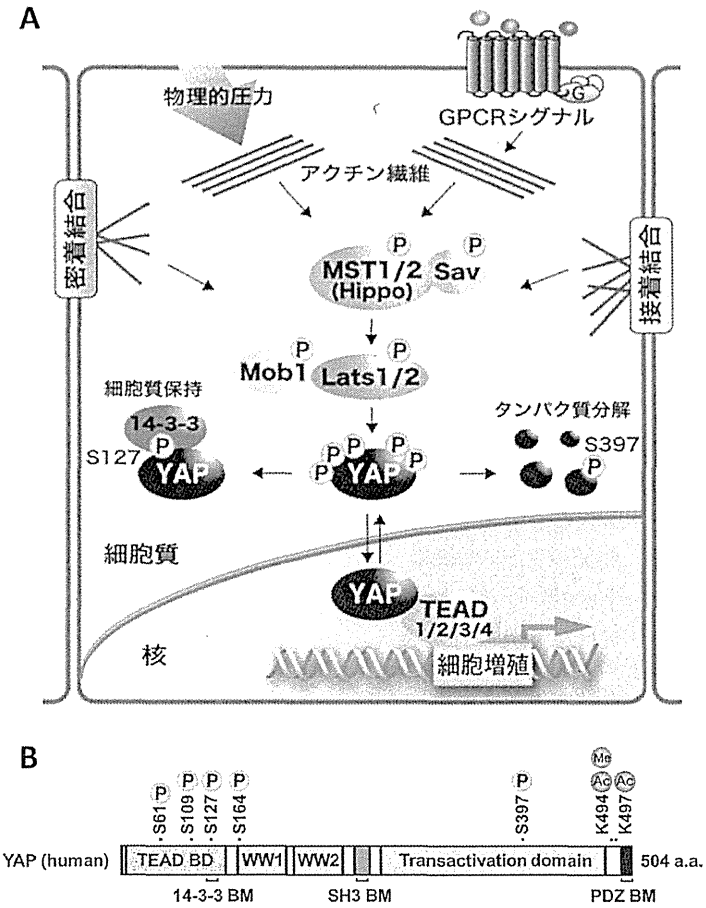

図2　Hippo 経路による YAP のリン酸化制御
(A) Hippo 経路の模式図．(B) YAP のドメイン構造．Hippo 経路による5か所のリン酸化部位 (P) と新たに同定されたアセチル化 (Ac) およびモノメチル化部位 (Me)．

とする遺伝子の発現を誘導する．中でも，YAP の機能を主に介在する転写因子は TEAD であり，TEAD は細胞増殖の促進や細胞死の抑制に関与する遺伝子群の発現を担っている．

Hippo 経路においてシグナル伝達経路としての中核をなすのは，セリン／トレオニンキナーゼの Mst1/2 と Lats1/2 によるキナーゼカスケードである．Mst1/2 は Lats1/2 をリン酸化して活性化させる．活性化された Lats1/2 は YAP の5か所のセリン残基をリン酸化する（図 2B）．127 番目のセリン残基がリン酸化されると，14-3-3 タンパク質がこの部位に直接結合することにより YAP を細胞質に保持する[4]．その結果，YAP の核内局在が抑制されて YAP 依存的な遺伝子発現が負に制御される．また，YAP の 397 番目のセリン残基が Lats1/2 によりリン酸化されると，ユビキチンリガーゼ複合体との相互作用が誘導され，YAP はユビキチン・プロテアソーム系依存的に分解される[5]．このように，Hippo 経路はリン酸化を介して YAP の細胞内局在と安定性を制御することで，YAP による細胞増殖や発がん性形質転換の誘導を抑制している．

Hippo 経路の主要構成因子は，ヒトから海綿動物に至る後生動物間において進化的にほぼ保存されている[6]．植物には保存されていないものの，一部の単細胞真核生物にまで保存されている点は興味深い．Hippo 経路の起源は出芽酵母における分裂期脱出制御分子群 (Mitotic Exit Network) や分裂酵母における隔壁形成分子群 (Septation Initiation Network) にあると考えられており，主要構成因子が保存されているだけでなく，シグナル伝達機構も類似している[7]．YAP 自体は酵母に保存されていないものの，非後生生物であるアメーバ型の真核単細胞生物 *Capsaspora owczarzaki* には保存されている[8]．この YAP ホモログも組織サイズ制御能力を保持することがショウジョウバエを用いた解析により示されている．このため，Hippo-YAP 経路は進化的に広く保存された細胞の増殖制御機構であるとみなすことができる．

4. 細胞の接触状態を感知するアクチン細胞骨格による YAP の活性制御

生体器官において血球系以外の細胞は隣接する細胞や周囲の細胞外基質と常に接触した状態にある．細胞による接触状態の感知は組織の恒常性維持に重要であり，その重要性は，非腫瘍性培養細胞株が接触阻害（contact inhibition）という高細胞密度時にみられる増殖停止機構を有することからも示唆される．Hippo 経路は細胞間の接触によって活性化され，接触阻害の分子機構として機能することが示されている[4]．特に，上皮細胞はさまざまな細胞間結合によって隣接した細胞と強固に接着している．上皮細胞間結合やそれによって形成される上皮細胞極性の維持は，細胞の腫瘍抑制機構の一つであり，それらが崩壊した細胞では YAP が活性化していることが示されている[1]．興味深いことに，Hippo 経路の上流制御因子として同定されている多くの分子が，密着結合，接着結合，頂端極性複合体の構成因子として知られている．

細胞は隣接した細胞に加えて細胞外基質にも接触しており，このような接触による外的な物理的圧力を感知して，増殖や遊走といったさまざまな細胞の挙動を制御している．アクチンなどの細胞内骨格がこのような物理的圧力の感知を担っているが，そのシグナルが YAP および TAZ を介して核内での遺伝子発現誘導に至ることが近年明らかになった[9]．接触する細胞外基質の剛性が高いときや細胞の形態が広がっている場合には，接着斑を介して細胞内のアクチン線維の張力が高まり，YAP および TAZ の活性化を誘導する．アクチン線維から YAP の活性化に至る分子機構は未解明な点が多いが，Hippo 経路依存的な機構と非依存的な機構が報告されている．興味深いことに，物理的圧力に加えて，G タンパク質共役型受容体（GPCR）シグナル伝達経路といった，アクチン線維の形成やストレスファイバーの形成を誘導する刺激も YAP の活性化を誘導することが報告された[10]．また，上皮細胞における接着結合の細胞質側にはアクチン線維が集積しており，密着結合によって形成される上皮細胞極性にはアクチン細胞骨格が必要である．これらのことから，細胞の接触状態に依存したアクチン細胞骨格の変化に応答して YAP の活性化状態を制御し，細胞は増殖や遊走，分化といった細胞機能を発揮していると考えられる．

5. アセチル化とメチル化による YAP の新たな制御機構

1) アセチル化による YAP の制御

上記のように，細胞質における YAP の制御機構は詳細に解析されているが，YAP が機能する核内での制御機構については不明な点が多い．我々はこの点に着目し，YAP の核内移行を誘導する刺激を利用して核内における YAP の制御機構を探索し，YAP が新たにアセチル化されることを見いだした[11]．解析の結果，① YAP の C 末端近傍の 2 か所のリシン残基（K494 と K497）がアセチル化修飾を受けること，② YAP のアセチル化が核内に局在するアセチル化酵素 CBP/p300 によって担われていること，③脱アセチル化を担う酵素は SIRT1 であること，④アセチル化部位の変異により YAP の転写活性化能が変化することを見いだした（図 3A）．CBP/p300 は YAP と同様に転写共役因子として機能することが知られており，また，SIRT1 もエピジェネティックな制御を介して遺伝子発現を調節することが知られている．このため，これらの酵素は YAP のアセチル化状態を制御して，YAP による遺伝子発現誘

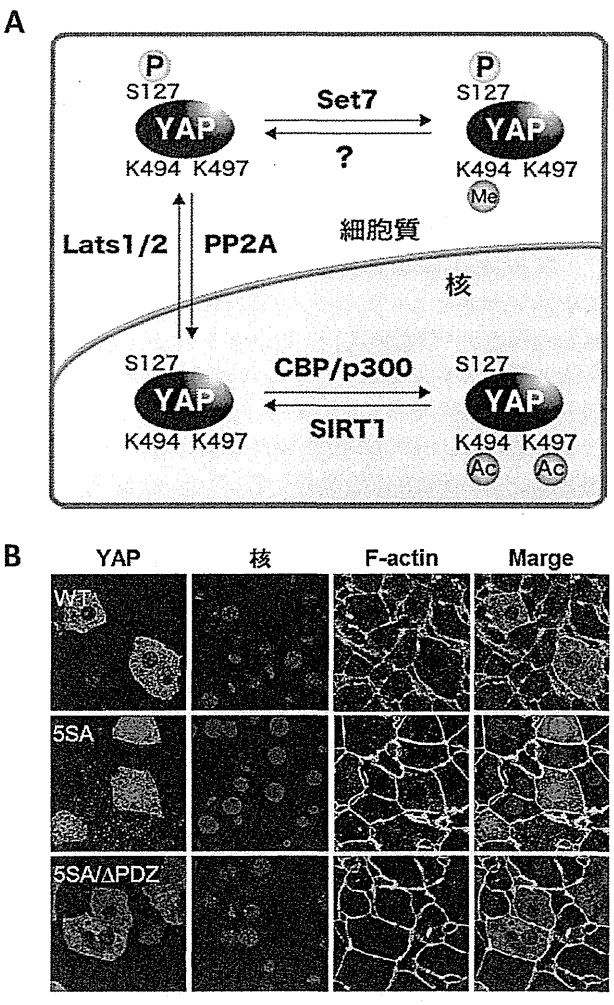

図 3　YAP の翻訳後修飾と細胞内局在制御
（A）YAP のリン酸化，アセチル化，モノメチル化修飾と触媒酵素．（B）野生型 YAP（上段）と変異型 YAP（中，下段）のマウス肝細胞内局在．

導を調節している可能性が考えられる．

2) モノメチル化による YAP の制御

YAP のアセチル化部位の一つである K494 は，ショウジョウバエからヒトに至るまで進化上高度に保存されているアミノ酸残基である．我々は Zaph らのグループとの共同研究により，YAP の K494 が新たにモノメチル化されることを明らかにした（図 3A）[12]．解析の結果，①メチル化酵素 Set7 が YAP のモノメチル化および培養線維芽細胞での細胞質への局在化に必要であること，②Set7 を欠損したマウスの腸管上皮において前駆細胞の増加を伴う形態異常が生じること，③この前駆細胞では YAP の核内局在が亢進し下流遺伝子群の発現が亢進することを見いだした．培養線維芽細胞において Set7 は主に細胞質に局在していることから，YAP のモノメチル化は細胞質で生じており，YAP を細胞質に保持するために機能していることが示唆される．また，Set7 欠損マウスで観察される表現型は Hippo 経路の破綻によって生じる表現型と類似している．これらの結果は，リン酸化修飾に加えて，モノメチル化修飾による YAP の機能制御も個体の組織恒常性維持において重要な役割を担っていることを示唆している．

3) アセチル化／モノメチル化部位の近傍に存在する PDZ-binding motif の機能

YAP のアセチル化／モノメチル化部位である K494 の C 末端側の数アミノ酸近傍に，PDZ-BM（PDZ-binding motif）が存在する．我々は最近，この PDZ-BM が生体マウス肝臓の肝実質細胞において，YAP の核内局在に必須であることを見いだした[13]（図 3B）．野生型の YAP（WT）は肝実質細胞において細胞質に局在するが，Hippo 経路によるリン酸化部位をアラニン残基に変異させた YAP（5SA）は核内に強く局在する．しかし，PDZ-BM を欠失した YAP（5SA/ΔPDZ）は核内に局在することはできない．YAP の細胞内局在を制御する分子の一つとして PDZ ドメインを有する ZO2（zonula occludens 2）が報告されている[14]．このため，YAP のアセチル化／モノメチル化は近傍の PDZ-BM の機能に影響を与え，ZO2 などの PDZ ドメイン含有タンパク質との相互作用を変化させることで YAP の細胞内局在を制御している可能性が考えられる．

リシン残基はアセチル化修飾とメチル化修飾を同時に受けることができないことから，リシン残基の修飾状態の変化はタンパク質の機能を切り替えるスイッチとして働く可能性がある．これまでに，ヒストン H3 の K9 がアセチル化とトリメチル化の修飾を受け，これらの修飾がクロマチン構造の変換のスイッチの役割を果たすことが知られている[15]．それゆえ，YAP における K494 のアセチル化とモノメチル化も YAP の機能を制御するスイッチとして働き，転写活性化能の調節や細胞内局在制御を担う可能性が考えられる．

6. おわりに

器官のサイズ制御機構は長い間不明であったが，近年の研究の進展により，器官サイズを制御する細胞内の分子機構（Hippo-YAP 経路）の実態と，個々の細胞が置かれている状況（情報）を細胞内へ伝達する分子機構（アクチン細胞骨格による接触情報の感知）が明らかとなりつつある．このような知見を基盤として，器官サイズ制御機構においていまだ不明な点の多い，器官レベルと細胞レベルの二つの階層間の隔たりを埋める分子機構の解明が期待される．

1) Yu, F.X. & Guan, K.L. (2013) *Genes Dev.*, 27, 355–371.
2) Dong, J., Feldmann, G., Huang, J., Wu, S., Zhang, N., Comerford, S.A., Gayyed, M.F., Anders, R.A., Maitra, A., & Pan, D. (2007) *Cell*, 130, 1120–1133.
3) Zender, L., Spector, M.S., Xue, W., Flemming, P., Cordon-Cardo, C., Silke, J., Fan, S.T., Luk, J.M., Wigler, M., Hannon, G.J., Mu, D., Lucito, R., Powers, S., & Lowe, S.W. (2006) *Cell*, 125, 1253–1267.
4) Zhao, B., Wei, X., Li, W., Udan, R.S., Yang, Q., Kim, J., Xie, J., Ikenoue, T., Yu, J., Li, L., Zheng, P., Ye, K., Chinnaiyan, A., Halder, G., Lai, Z.C., & Guan, K.L. (2007) *Genes Dev.*, 21, 2747–2761.
5) Zhao, B., Li, L., Tumaneng, K., Wang, C.Y., & Guan, K.L. (2010) *Genes Dev.*, 24, 72–85.
6) Hilman, D. & Gat, U. (2011) *Mol. Biol. Evol.*, 28, 2403–2417.
7) Hergovich, A. & Hemmings, B.A. (2012) *Semin. Cell Dev. Biol.*, 23, 794–802.
8) Sebe-Pedros, A., Zheng, Y., Ruiz-Trillo, I., & Pan, D. (2012) *Cell Rep.*, 1, 13–20.
9) Dupont, S., Morsut, L., Aragona, M., Enzo, E., Giulitti, S., Cordenonsi, M., Zanconato, F., Le Digabel, J., Forcato, M., Bicciato, S., Elvassore, N., & Piccolo, S. (2010) *Nature*, 474, 179–183.
10) Yu, F.X., Zhao, B., Panupinthu, N., Jewell, J.L., Lian, I., Wang, L.H., Zhao, J., Yuan, H., Tumaneng, K., Li, H., Fu, X. D., Mills, G.B., & Guan, K.L. (2012) *Cell*, 150, 780–791.
11) Hata, S., Hirayama, J., Kajiho, H., Nakagawa, K., Hata, Y., Katada, T., Furutani-Seiki, M., & Nishina, H. (2012) *J. Biol. Chem.*, 287, 22089–22098.
12) Oudhoff, M.J., Freeman, S.A., Couzens, A.L., Antignano, F., Kuznetsova, E., Min, P.H., Northrop, J.P., Lehnertz, B., Barsyte-Lovejoy, D., Vedadi, M., Arrowsmith, C.H., Nishina, H., Gold, M.R., Rossi, F.M., Gingras, A.C., & Zaph, C. (2013) *Dev. Cell*, 26, 188–194.
13) Shimomura, T., Miyamura, N., Hata, S., Miura, R., Hirayama, J., & Nishina, H. (2014) *Biochem. Biophys. Res. Commun.*, 443, 917–923.
14) Oka, T., Remue, E., Meerschaert, K., Vanloo, B., Boucherie, C., Gfeller, D., Bader, G.D., Sidhu, S.S., Vandekerckhove, J., Gettemans, J., & Sudol, M. (2010) *Biochem. J.*, 432, 461–472.
15) Sims, R.J., 3rd, Nishioka, K., & Reinberg, D. (2003) *Trends Genet.*, 19, 629–639.

著者寸描

●畠　星治（はた　しょうじ）

日本学術振興会特別研究員（PD），東京大学大学院薬学系研究科生理化学教室所属．理学博士．

■略歴　1983年埼玉県に生る．2006年東京薬科大学生命科学部卒業．11年東京医科歯科大学大学院生命情報科学部博士課程修了．08～11年日本学術振興会特別研究員（DC1）．11～13年東京医科歯科大学難治疾患研究所特任助教．13年より現職．

■研究テーマと抱負　腫瘍抑制機構の解明をHippo経路の観点から行っている．14年3月からドイツ・ハイデルベルク大学Elmar Schiebel研究室との共同研究のため，長期の渡独．ドイツ留学を楽しみたい．

■ウェブサイト　http://www.f.u-tokyo.ac.jp／~seiri/

■趣味　料理，ソフトテニス．

肝形成および肝癌における Hippo-YAPシグナル経路の役割

Roles of Hippo-YAP signaling pathway for liver formation and liver cancer

千葉恭敬(写真)　仁科博史
Takanori CHIBA[1,2] and Hiroshi NISHINA[1]
東京医科歯科大学難治疾患研究所発生再生生物学分野[1]，同大学院医歯学総合研究科分子内分泌代謝学分野[2]

◎肝は糖質・蛋白質・脂質などの代謝をはじめ，有害物質の解毒や胆汁酸の生成・分泌など多岐にわたる機能を有しており，生体の恒常性維持に必要不可欠な器官である．そのため生命活動を維持するのに十分な肝機能を発揮できるように，肝はつねに適切な器官サイズ制御を受けている．近年，細胞内情報伝達経路のひとつであるHippoシグナル経路が，転写共役因子であるYAPの活性制御を介してマウスの肝サイズを調節していることが明らかとなった．また，Hippo-YAPシグナル経路は肝癌発症や肝内胆管の発生にも関与することも見出されている．さらに最近では，ヒトの肝癌発症や小児の胆道形成に対するHippo-YAPシグナル経路の関与を示唆する臨床的な知見も数多く報告されている．本稿ではこのような最近の知見を踏まえ，マウスおよびヒトの肝におけるHippo-YAPシグナル経路の役割について紹介する．

Key word：Hippo，YAP，肝サイズ，肝癌，胆管形成

肝は個体の生命維持に必須の器官であり，その機能不全は個体の死に直結する．肝機能不全をきたす代表的な疾患は肝癌(肝細胞癌，胆管細胞癌，肝芽腫など)である．肝癌は，肝を構成する細胞が腫瘍性に増殖することにより発症する．通常，肝を構成する細胞は適切な数を保つように調節されているが，遺伝子変化などにより癌化能力を獲得すると，こうした細胞数の制御から外れ無秩序に増殖し続け，最終的に肝癌を発症する．これまで肝の細胞数を調節するメカニズムは不明であったが，近年になり徐々に解明されつつある．

Hippo-YAPシグナル経路

Hippoシグナル経路はmammalian Ste20-like kinase 1/2(MST1/2)，large tumor suppressor 1/2(LATS1/2)，salvador 1(SAV1)，mps one binder 1a/1b(MOB1A/1B)により構成されており，Hippoシグナル経路は転写共役因子であるYAPをリン酸化することにより負に制御する(図1)．

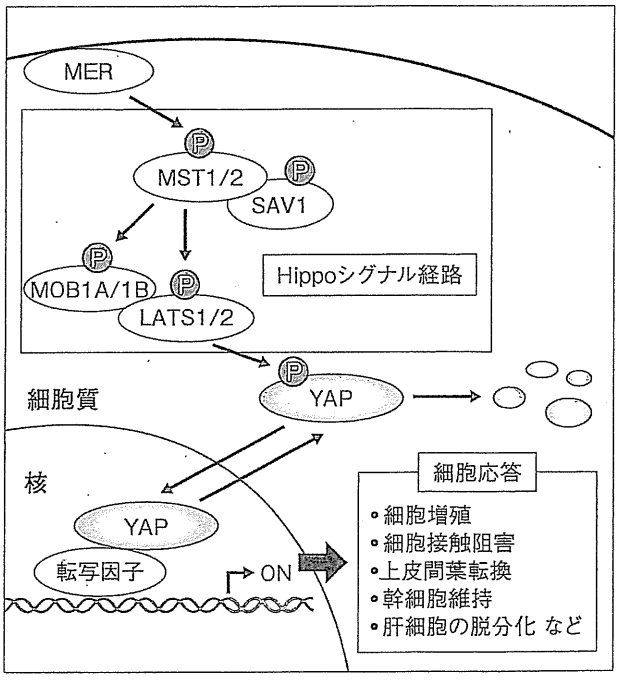

図1　種々の細胞応答を制御するHippo-YAPシグナル経路
MERはHippoシグナル経路の上流分子であり，Hippoシグナル経路はYAPを負に制御する．YAPは種々の細胞応答を引き起こす遺伝子の発現を制御する．

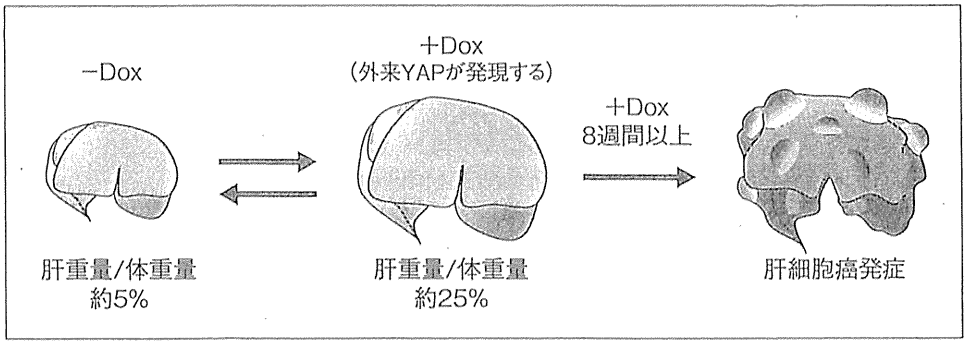

図 2　外来YAP発現誘導による肝のサイズ増大と肝癌発症
Dox 依存的に外来 YAP を過剰発現する Tg マウスの肝．体重に占める肝重量の割合は通常 5%程度であるが，Dox を投与すると約 25%に増加する．しかし，Dox の投与を中止すると肝のサイズは元に戻る．一方，8 週間以上 Dox を持続的に投与すると肝細胞癌が生じる．

Hippoシグナル経路によってリン酸化されたYAPは細胞質に保持または分解される．一方，リン酸化を受けていないYAPは活性型として核内で転写因子と結合し，YAP依存的な遺伝子発現を誘導する．Hippoシグナル経路の代表的な上流分子として，ヒトⅡ型神経線維鞘腫の原因遺伝子として同定された *neurofibromatosis type 2*(*Nf2*)遺伝子がコードする蛋白質merlin(MER)が知られている．Hippo-YAPシグナル経路は，細胞レベルの機能として細胞増殖，細胞接触阻害(contact inhibition)，上皮間葉転換(epithelial mesenchymal transition)，幹細胞維持，および肝細胞の脱分化などにかかわることが報告されている[1-3]．

Hippo-YAPシグナル経路による成体マウスの肝サイズ制御と発癌抑制

2007年にDongらは，ドキシサイクリン(Dox)依存的に肝でYAPを過剰発現するトランスジェニック(Tg)マウスを作出した[4](図2)．本TgマウスにおいてDoxを投与すると，肝のサイズが野生型マウスと比較して約5倍にまで増加した．肝のサイズは“細胞の数”と“細胞の大きさ”により規定されるが，本Tgマウスはおもに“細胞の数”の増加により肝のサイズが増大していることが明らかとなった．興味深いことに，この増大した肝のサイズはDox投与を中止すると元に戻る．すなわち，YAPによる肝のサイズ制御は可逆的であることが示された．一方，8週間以上の長期間にわたりDoxを投与し続けた本Tgマウスは肝細胞癌を発症した．以上の結果から，YAPは“細胞の数”を調節することにより肝のサイズを制御しており，このサイズ制御の長期間にわたる破綻が肝癌を惹起したと考えられる．

2009年以降には，Hippoシグナル経路の構成分子を肝特異的にノックアウト(KO)したマウスの解析がつぎつぎと報告されてきた(表1)．MST1とMST2の両者の肝特異的なKOマウスは野生型のマウスと比較して生後2カ月の段階で肝のサイズが5倍程度まで増大し，生後3～6カ月において肝細胞癌を発症することが複数のグループにより示された[5-7]．SAV1の肝特異的なKOマウスは生後4カ月において肝のサイズが1.5倍程度に増大し，生後12～14カ月ごろに肝細胞癌や胆管細胞癌を発症する[6,8]．さらに，肝においてMOB1A/1Bが欠損したマウスは生後17カ月ごろに肝癌を発症する[9]．また，Hippoシグナル経路の上流分子であるMERの肝特異的なKOマウスは肝のサイズが5～7倍程度に増大し，生後7～12カ月において肝細胞癌や胆管細胞癌を発症する[10,11]．以上のように，Hippoシグナル経路の構成分子や上流分子のKOマウスはYAP Tgマウスと同様に肝のサイズが増大し肝癌を発症することが明らかとなった．

YAPによる発生期のマウス肝形成の制御

マウス肝の発生は胎生8日(E8)ごろに，前腸内胚葉に肝の予定領域が決定されることよりはじまる．肝の発生の進行に伴い，肝内胆管の形成が起

表 1　Hippo-YAPシグナル経路構成分子の遺伝子改変マウスの表現型

分子	遺伝子改変マウス	肝のサイズ増大	肝癌形成	文献
MER	*Nf2*$^{+/-}$	−	+	23)
	Alb-Cre Nf2$^{f/f}$	+	+	10,11)
MST1/2	*Mst1*$^{-/-}$*Mst2*$^{+/-}$*1	+	+	5)
	Mst1$^{+/-}$*Mst2*$^{-/-}$*2	+	+	5,24)
	Alb-Cre Mst1$^{-/-}$*Mst2*$^{f/f}$	+	+	5)
	Ad-Cre Mst1$^{-/-}$*Mst2*$^{f/-}$	+	+	5)
	Alb-Cre Mst1$^{f/f}$*Mst2*$^{f/f}$	+	+	6)
	Alb-Cre Mst1$^{-/-}$*Mst2*$^{f/-}$	+	未記載	7)
	CAGGS-CreER Mst1$^{-/-}$*Mst2*$^{f/-}$	+	+	7)
SAV1	*Sav*$^{+/-}$	−	+	8)
	Alb-Cre Sav1$^{f/f}$	+	+	6,8)
	MMTV-Cre Sav1$^{f/f}$	未記載	+	6)
	CAGGS-Cre ER Sav1$^{f/f}$	未記載	+	6)
MOB1A/1B	*Mob1a*$^{\Delta/\Delta}$*Mob1b*$^{tr/+}$*3	未記載	+	9)
YAP	*Tg:ApoE/tTA*	+	+	4)
	Tg:LAP/tTA	+	未記載	25)

*1：Mst2 のアレル欠失が生じると表現型が観察される．
*2：Mst1 のアレル欠失が生じると表現型が観察される．
*3：Mob1b のアレル欠失が生じると表現型が観察される．

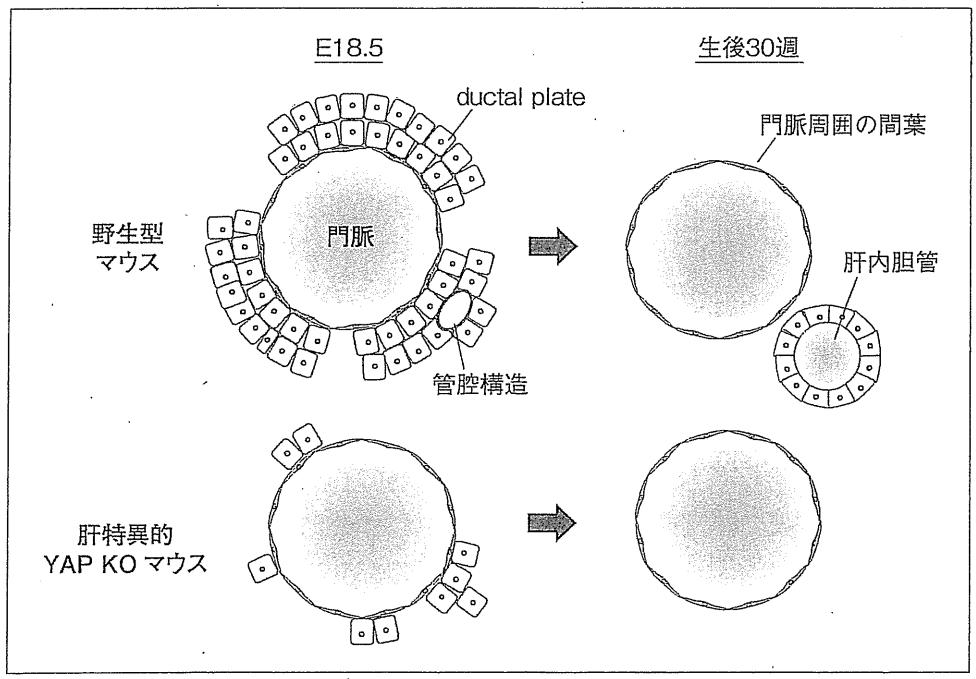

図 3　肝特異的YAP KOマウスにおける肝内胆管発生異常の解析
上：野生型マウスにおける正常な肝内胆管形成過程．E18.5 では ductal plate により管腔構造が形成され，生後 30 週には正常な肝内胆管が形成される．
下：肝特異的 YAP 欠損マウスにおける肝内胆管形成異常．E18.5 では ductal plate の形態異常が生じ，管腔構造ほとんど形成されていなかった．また，生後 30 週では肝内胆管は認めなかった．

こる．肝内胆管の形成過程としては通常，E15.5 ごろに門脈に隣接する胆管前駆細胞から胆管板(ductal plate)が形成され，出生前に ductal plate の一部が管腔構造を呈する．その後，管腔構造は門脈周囲の間葉に取り込まれ肝内胆管となり，残りの ductal plate は生後に退行する．

表 2　ヒト肝癌とHippo-YAPシグナル経路構成分子のかかわり

分子	内容	文献
MST	21 例中 13 例(62%)の肝細胞癌で，切断型 MST1(活性型 MST1)が減少していた	5)
	35 例中 30 例(86%)の肝細胞癌で，リン酸化 MST1(活性型 MST1)が減少していた	13)
LATS	7 例すべての非癌部で LATS は検出されたが，7 例中 4 例(57%)の肝細胞癌で LATS は検出されなかった	14)
MOB1	21 例中 15 例(71%)の肝細胞癌で，リン酸化 MOB1(活性型 MOB1)が減少していた	5)
YAP	*YAP* 遺伝子座を含むゲノム領域(11q22)が増幅されている肝細胞癌を認めた	15)
	33 例の B 型肝炎ウイルス(HBV)陽性患者の肝細胞癌の解析結果では非癌部と比較して癌部の YAP の mRNA 発現は著明に上昇していた．YAP と HBx(HBV がコードする蛋白質)の両 mRNA の発現レベルには正の相関があった	16)
	20 例中 13 例(65%)の肝細胞癌で YAP の発現は亢進していた	4)
	177 例中 110 例(62%)の肝細胞癌で YAP の発現を認め，大部分は YAP は核に存在していた．YAP 陰性と比較して，YAP 陽性肝細胞癌患者は血清 AFP 値が高く，癌の分化度が低かった．また，YAP 陰性と比較して，YAP 陽性肝細胞癌患者の生存率は低かった	17)
	70 例中 47 例(67%)の肝細胞癌では YAP は強く発現していた．予後のよい患者と比較し，予後の悪い患者の肝細胞癌は核局在の YAP や血清 AFP 値の増加を認めた	18)
	115 例中 63 例(54%)の肝細胞癌で，YAP は強く発現していた	19)
	21 例中 7 例(33%)の肝細胞癌で，リン酸化 YAP(不活性型 YAP)は減少していた	5)
	70 例の肝細胞癌，16 例の胆管細胞癌，22 例の肝芽腫の大部分で YAP は核に存在していた	14)
	103 例中 67 例(65%)の肝細胞癌，62 例中 61 例(98%)の胆管細胞癌，94 例中 80 例(85%)の肝芽腫で YAP は核に存在していた	20)
	YAP 陰性と比較して，YAP 陽性肝細胞癌患者は血清 AFP 値が高く，癌の分化度が低かった．また，YAP 陰性と比較して，YAP 陽性肝細胞癌患者の生存率は低かった	21)

発生期の肝形成における YAP の機能に関してはこれまでに全身性 YAP KO マウスが作出されたが，E8.5 ごろに個体の発生が停止してしまうため肝の評価が困難であった[12]．そこで Zhang らは肝特異的に YAP を KO することにより致死を回避することに成功し，胎仔や成体の肝の評価を行った[11]．その結果，本マウスは E18.5 において ductal plate による管腔構造の形成はほとんど認められず，生後30週では正常な肝内胆管は形成されないことが示された(図 3)．また，本マウスの成体は血清ビリルビン値や alanine aminotransferase(ALT)値が上昇しており，さらに肝の線維化をきたしていた．以上のことから，YAP はマウスの肝内胆管の形成に必要であることが明らかとなった．

Hippo-YAPシグナル経路による ヒト肝癌発症とヒト胆道形成の制御

近年，マウスの知見と同様に，ヒトにおいても肝癌発症に Hippo-YAP シグナル経路が関与していることが明らかにされている(表 2)．Hippo-YAP シグナル経路が肝癌発症に関与する際には，肝癌細胞において Hippo シグナル経路が不活性化されている，あるいは YAP が活性化されていると考えられる．ヒト肝癌における Hippo シグナル経路の不活性化については，これまでに MST，LATS，ならびに MOB1 に関する報告がなされている．たとえば，MST に関しては 21 例中 13 例(62%)および 35 例中 30 例(86%)のヒト肝細胞癌では非癌部と比較して活性型 MST1 が減少していることが示された[5,13]．また，LATS に関しては 7 例中 4 例(57%)のヒト肝癌において LATS 蛋白質が検出されないことが報告されている[14]．さらに MOB に関しては，21 例中 15 例(71%)のヒト肝細胞癌では非癌部と比較して活性型 MOB1 が減少していることが示されている[5]．

2006 年にはヒト肝細胞癌において *YAP* 遺伝子座を含むゲノム領域(11q22)が増幅されていることが報告され，YAP がヒト肝細胞癌発症に関与することが示唆された[15]．以降，今日までにヒト肝癌と YAP に関する報告はつぎつぎとなされており，ヒト肝細胞癌では非癌部と比較して YAP

のmRNAや蛋白質の発現レベルが亢進していることが示された[4,16-19]．さらに，ヒト肝細胞癌ではリン酸化を受けた不活性型のYAPが減少していることや，ヒト肝細胞癌，胆管細胞癌，および肝芽腫ではYAPは活性型として，おもに核に存在していることも示された[5,14,17,19,20]．このようにヒト肝癌においてYAPの発現，活性，ならびに核局在の割合が亢進していることが明らかとなってきている．

また，ヒト肝細胞癌の分化度や肝細胞癌患者の血清α-fetoprotein(AFP)値および予後に関する興味深い報告がある．Xuらは，YAP陰性の患者と比較してYAP陽性の肝細胞癌患者は血清AFP値が高いことや癌の分化度が低いことを示した[17]．さらに，YAP陽性の肝細胞癌患者では生存率が有意に低く，5年生存率はYAP陰性の患者は58%であるのに対し，YAP陽性の患者は36%に減少することも報告した．同様にHanらも，YAP陰性の患者と比較して，YAP陽性の肝細胞癌患者では血清AFP値が高いこと，癌の分化度が低いこと，生存率が低いことを示した[21]．以上のように，ヒト肝癌においてもHippo-YAPシグナル経路は肝癌発症の一因を担っていること，YAPは予後マーカーとなることが示唆された．

一方，ヒト胆道の形成とYAPに関する報告もなされている．胆道閉鎖症(BA)は新生児期から乳児期早期に発症する胆汁うっ滞性疾患のひとつであり，胆管の閉塞により重篤な肝障害を引き起こし，早期診断・早期治療が行われなければ死に至る疾患である．2014年にGurdaらはBA以外の原因による胆汁うっ滞性疾患の患児との比較解析によりBAの患児の肝組織では胆管上皮細胞のYAP発現が有意に亢進していることを見出した[22]．これにより，小児の胆汁うっ滞性疾患の鑑別診断を行うにあたりYAPがBAの診断の補助として有用であることが示された．

おわりに

2003年にショウジョウバエにおいて器官サイズを制御するシグナル伝達経路として，Hippo-YAPシグナル経路が同定された．その後10年の間に，マウスを用いた解析によりHippo-YAPシグナル経路の多様な役割が明らかにされてきた．近年ではヒトにおいても，肝癌のみならず卵巣癌や前立腺癌などでHippo-YAPシグナル経路が破綻していることが報告されている[1]．わが国では1981年以降，悪性新生物は死因の第一位であり，その死亡率は増加の一途をたどっている．そのため，今後はHippo-YAPシグナル経路の分子機構の知見を診断や治療に結びつけ，新規癌治療薬開発などが行われていくことが期待される．

謝辞：今回の執筆にあたり多大なご協力をいただいた東京医科歯科大学大学院医歯学総合研究科分子内分泌代謝学分野の小川佳宏先生に深く感謝致します．

文献

1) Harvey, K. F. et al.: *Nat. Rev. Cancer*, **13**: 246-257, 2013.
2) Zhao, B. et al.: *Nat. Cell. Biol.*, **13**: 877-883, 2011.
3) Yimlamai, D. et al.: *Cell*, **157**: 1324-1338, 2014.
4) Dong, J. et al.: *Cell*, **130**: 1120-1133, 2007.
5) Zhou, D. et al.: *Cancer Cell*, **16**: 425-438, 2009.
6) Lu, L. et al.: *Proc. Natl. Acad. Sci. USA*, **107**: 1437-1442, 2010.
7) Song, H. et al.: *Proc. Natl. Acad. Sci. USA*, **107**: 1431-1436, 2010.
8) Lee, K. P. et al.: *Proc. Natl. Acad. Sci. USA*, **107**: 8248-8253, 2010.
9) Nishio, M. et al.: *J. Clin. Invest.*, **112**: 4505-4518, 2012.
10) Benhamouche, S. et al.: *Genes. Dev.*, **24**: 1718-1730, 2010.
11) Zhang, N. et al.: *Dev. Cell*, **19**: 27-38, 2010.
12) Morin-Kensicki, E. M. et al.: *Mol. Cell. Biol.*, **26**: 77-87, 2006.
13) Diego. et al.: *Gastroenterology*, **130**: 1117-1128, 2006.
14) Li, H. et al.: *Liver Int.*, **32**: 38-47, 2012.
15) Zender, L. et al.: *Cell*, **125**: 1253-1267, 2006.
16) Zhang, T. et al.: *Hepatology*, **56**: 2051-2059, 2012.
17) Xu, M. Z. et al.: *Cancer*, **115**: 4576-4585, 2009.
18) Felix, D. et al.: *Gastroenterology*, **144**: 1530-1542, 2013.
19) Zhao, B. et al.: *Genes Dev.*, **21**: 2747-2761, 2007.
20) Tao, J. et al.: *Gastroenterology*, 2014, May 14.(Epub ahead of print)
21) Han, S. X. et al.: *J. Immunol. Res.*, 2014, Apr. 22.(Epub ahead of print)
22) Gurda, G. T. et al.: *Hum. Pathol.*, **45**: 1057-1064, 2014.
23) McClatchey, A. I. et al.: *Genes Dev.*, **12**: 1121-1133, 1998.
24) Avruch, J. et al.: *Br. J. Cancer*, **104**: 24-32, 2011.
25) Camargo, F. D. et al.: *Curr. Biol.*, **17**: 2054-2060, 2007.

The American Journal of Pathology, Vol. 184, No. 8, August 2014

ELSEVIER

The American Journal of
PATHOLOGY

ajp.amjpathol.org

GASTROINTESTINAL, HEPATOBILIARY, AND PANCREATIC PATHOLOGY

Semaphorin 3E Secreted by Damaged Hepatocytes Regulates the Sinusoidal Regeneration and Liver Fibrosis during Liver Regeneration

Tomoki Yagai,* Atsushi Miyajima,* and Minoru Tanaka[†‡]

From the Laboratories of Cell Growth and Differentiation and Stem Cell Regulation,[†] Institute of Molecular and Cellular Biosciences, The University of Tokyo, Tokyo; and the Department of Regenerative Medicine,[‡] Research Institute, National Center for Global Health and Medicine, Tokyo, Japan*

Accepted for publication
April 28, 2014.

Address correspondence to Minoru Tanaka, Ph.D., Laboratory of Stem Cell Regulation, Institute of Molecular and Cellular Biosciences, The University of Tokyo, 1-1-1 Yayoi, Bunkyo-ku, Tokyo 113-0032, Japan. E-mail: tanaka@iam.u-tokyo.ac.jp.

The liver has a remarkable capacity to regenerate after injury. Although the regulatory mechanisms of hepatocytic regeneration have been a subject of intense study, the dynamism of the sinusoids, specialized blood vessels in the liver, remains largely unknown. Transient activation of hepatic stellate cells and hepatic sinusoidal endothelial cells, which constitute the sinusoids, contributes to liver regeneration during acute injury, whereas their sustained activation causes liver fibrosis during chronic injury. We focused on understanding the association between damaged hepatocytes and sinusoidal regeneration or liver fibrogenesis using a carbon tetrachloride–induced liver injury mouse model. Damaged hepatocytes rapidly expressed semaphorin 3E (Sema3e), which induced contraction of sinusoidal endothelial cells and thereby contributed to activating hepatic stellate cells for wound healing. In addition, ectopic and consecutive expression of Sema3e in hepatocytes by the hydrodynamic tail-vein injection method resulted in disorganized regeneration of sinusoids and sustained activation of hepatic stellate cells. In contrast, liver fibrosis ameliorated in *Sema3e*-knockout mice compared with wild-type mice in a chronic liver injury model. Our results indicate that Sema3e, secreted by damaged hepatocytes, affects sinusoidal regeneration in a paracrine manner during liver regeneration, suggesting that Sema3e is a novel therapeutic target in liver fibrogenesis. *(Am J Pathol 2014, 184: 2250–2259; http://dx.doi.org/10.1016/j.ajpath.2014.04.018)*

The liver has a remarkable capacity to regenerate from surgical resection and damage caused by various insults, such as toxic chemicals and viral infection. Many injuries cause death of hepatocytes, which are liver parenchymal cells, followed by compensatory proliferation of the remaining hepatocytes to regenerate.[1] Therefore, the mechanisms of liver regeneration are focused on hepatocytes,[2,3] whereas the regenerative process of sinusoids, unique capillary vessels in the liver, remains largely unknown. The hepatic sinusoid is composed of fenestrated sinusoidal endothelial cells (SECs) and hepatic stellate cells (HSCs). In general, the process of liver regeneration after injury is accompanied by sinusoid fibrogenesis. Although transient fibrogenesis is beneficial for wound healing by providing mechanical stability and a scaffold for hepatocytic regeneration,[4] prolonged fibrogenesis during chronic hepatitis often leads to the accumulation of extracellular matrix (ECM), resulting in nodule formation and alterations in hepatic function and blood flow. Therefore, liver fibrosis is a pathologic sign that results in severe hepatic diseases, such as cirrhosis and carcinogenesis.[5] Previous studies have revealed that HSCs, characteristic pericytes that line the hepatic sinusoid, are a key cellular source for the ECM and that activated HSCs acquire myofibroblastic characteristics by secreting excess ECM protein, such as collagen types I and III.[6] In addition, SECs and HSCs cooperate to maintain the sinusoidal environment. For example, vascular endothelial growth factor (VEGF) secreted by HSCs maintains SEC homeostasis by preventing their capillarization.[7] Conversely, SECs revert activated HSCs to a

Supported in part by Grants-in-Aid for Scientific Research 22590719 and 22118006 from the Japan Society for the Promotion of Science, Japan (A.M. and M.T.).

Disclosures: None declared.

Copyright © 2014 Published by Elsevier Inc. on behalf of the American Society for Investigative Pathology.
http://dx.doi.org/10.1016/j.ajpath.2014.04.018

quiescent status via nitric oxide synthesis.[8] These observations suggest that the reciprocal cell-to-cell communication between SECs and HSCs is critical for sinusoidal regeneration and liver fibrosis after liver injury and that SEC angiogenic factors could be the regulators of liver fibrogenesis through indirect activation of HSCs. Because liver injury is accompanied by inflammation and hepatocytic insults, inflammatory cells are involved in sinusoidal fibrogenesis.[9] In addition, molecules secreted from damaged hepatocytes contribute to the compensatory proliferation of surrounding hepatocytes.[10,11] However, whether there is a direct association between damaged hepatocytes and sinusoidal regeneration or liver fibrogenesis is currently unknown.

We found that semaphorin 3E (Sema3e) is up-regulated by 3,5-diethoxycarbonyl-1,4-dihydrocollidine feeding in a mouse model of chronic hepatitis.[12,13] Sema3e is a secretory protein that belongs to the class 3 semaphorin family[14] and plays a neurogenic and angiogenic repulsive role in development.[15,16] The receptors for semaphorins are plexins and neuropilins, and Sema3e specifically binds to plexin D1 (Plxnd1).[17] Sakurai et al[18] reported that Sema3e/Plxnd1 signaling initiates the antiangiogenic response by regulating Arf6 and R-Ras, inhibiting endothelial tip cell adhesion to the ECM, and retracting filopodia. Moreover, the Sema3e/Plxnd1 axis interferes with VEGF and VEGF receptor (VEGFR)-2 signaling via a feedback mechanism.[19] Indeed, Sema3e/Plxnd1 signaling plays an essential role in development because *Sema3e*-knockout (KO) mice display aberrant vascularization of intersomitic blood vessels.[17] However, the involvement of Sema3e/Plxnd1 signaling in liver regeneration and pathogenesis remains largely unknown. In this study, we focused on the mechanisms of sinusoidal regeneration after liver injury and found that Sema3e produced by damaged hepatocytes activates SECs via Plxnd1 and thereby plays a critical role in sinusoidal regeneration and liver fibrosis.

Materials and Methods

Mice

C57BL/6 mice were obtained from CLEA Japan (Tokyo, Japan). *Sema3e*-KO mice were provided by Dr. Yutaka Yoshida (Cincinnati Children's Hospital Medical Center, Cincinnati, OH).[17] The littermates were subjected to carbon tetrachloride (CCl_4)—induced liver fibrosis. All animal experiments were performed in accordance with our institutional guidelines.

Induction of CCl_4-Induced Acute Liver Injury and Liver Fibrosis

Acute liver injury was induced by single i.p. injection of CCl_4. CCl_4 (Wako Pure Chemical, Osaka, Japan) was diluted in corn oil (Wako) to 20% and injected into mice at a dose of 1 mL/kg of CCl_4. Liver fibrosis was induced by repeated injection of CCl_4, twice per week for 4 weeks. Livers were harvested 3 days after the final CCl_4 injection.

H&E and Sirius Red Staining

Liver cryosections (8 μm) were mounted on glass slides and fixed with Zamboni fixative solution for 10 minutes for immunostaining. The fixed sections were incubated with 5% skim milk (w/v) in phosphate-buffered saline and then incubated with primary antibodies, followed by secondary antibodies. The antibodies used in this study are listed in Table 1. Images were captured using Observer Z1 with an AxioCam HRc (Zeiss, Oberkochen, Germany). The hematoxylin and eosin (H&E) staining was performed after immunostaining in some specific experiments as stated later. The cover glass on enclosed sections was eliminated carefully with adequate phosphate-buffered saline (Wako) and then stained with H&E (Muto Pure Chemicals, Tokyo, Japan). Sirius Red staining was performed followed by Bouin's solution (Sigma-Aldrich, St. Louis, MO) fixation, as described previously. In brief, nuclei were stained with Weigert's iron hematoxylin (Wako) and then stained with collagen and Direct Red 80 (Sigma-Aldrich).

RT-PCR and Real-time RT-PCR

Total RNA was isolated from mouse livers or hepatic cells using TRIzol reagent (Invitrogen). Reverse transcription to cDNA templates was performed using random primers and a High-Capacity cDNA Reverse-Transcription Kit (Applied Biosystems, Foster City, CA). Real-time RT-PCR experiments were conducted with a LightCycler 480 system and Universal Probe Library (Roche Diagnostics, Indianapolis, IN). The mouse *ACTB* gene assay in ProbeLibrary was used as the normalization control. The sequence information for the primer pairs used is listed in Table 2. Probes #63 and #27 were used for *Sema3e* and *Plxnd1*, respectively. Sema3e primers were used for experiments by analyzing the Sema3e expression. Sema3e vector primers were used to construct the expression vector.

Table 1 Antibodies Used in the Study

Protein	Supplier
Semaphorin 3E (Sema3e)	Abgent (San Diego, CA)
Stabilin-2 (Stab-2)	Nonaka et al[20]
CD45	BD Biosciences (San Diego, CA)
Nerve growth factor receptor (NGFR, p75NTR)	R&D Systems (Minneapolis, MN)
Actin, α_2, smooth muscle, aorta (α-SMA)	Abcam (Cambridge, MA)
CD16/CD32 (Fcγ III/II Receptor)	BD Biosciences
Ki-67	eBioscience (San Diego, CA)
Collagen I	AbD Serotec (Kidlington, UK)
Phalloidin	Invitrogen (Carlsbad, CA)
GAPDH	Merck Millipore (Billerica, MA)

α-SMA, α-smooth muscle actin; GAPDH, glyceraldehyde-3-phosphate dehydrogenase; p75NTR, p75 low-affinity neurotrophic growth factor receptor.

Table 2 Primer Sequences Used for This Study

Gene	Sense primer sequence	Antisense primer sequence
Sema3e	5′-GGGGCAGATGTCCTTTTGA-3′	5′-AGTCCAGCAAACAGCTCATTC-3′
Plxnd1	5′-CTGGATGTCCATCTGCATGT-3′	5′-CAGGAAGAACGGCTCACCTA-3′
Construction for *Sema3e* expression vector	5′-AGCTAGCCCCTGGAGGGAAGTACTAA-3′	5′-GTCGACTCCTAGGTTCCTCAGCCGCC-3′

Cell Isolation

A single-cell suspension was obtained from the liver by a modified collagenase perfusion method, as described previously.[21] In brief, liver specimens were perfused with a basic perfusion solution containing 0.5 g/L of collagenase-Yakult (Yakult Pharmaceutical Industry Co. Ltd., Tokyo, Japan) and 50 mg/L of DNase I (Sigma-Aldrich). The digested liver was passed through a 70-μm cell strainer. After centrifugation at 60 × *g* for 1 minute, the precipitated cells were used as hepatocytes after Percoll (GE Healthcare, Piscataway, NJ) density centrifugation. The supernatant was transferred to a new tube and centrifuged at 120 × *g* for 2 minutes repeatedly until no pellet was visible. The final supernatant was centrifuged at 340 × *g* for 5 minutes, and the precipitated cells were used as non-parenchymal cells for cell isolation. Aliquots of cells were blocked with anti-FcγR antibody, co-stained with fluorescence- and/or biotin-conjugated antibodies, and then incubated with allophycocyanin-conjugated streptavidin (BD Biosciences, San Diego, CA) if needed. The samples were sorted by Moflo XDP (Beckman-Coulter, Fullerton, CA) or auto-MACS pro (Miltenyi Biotec, Bergisch Gladbach, Germany) with anti-allophycocyanin microbeads. Dead cells were excluded by propidium iodide staining.

Primary Culture of Hepatocytes and SECs

Primary hepatocytes separated by Percoll were seeded in type I collagen–coated 6-well dishes (BD Biosciences) at 5 × 10^5 per well with William's Medium E (Life Technologies, Carlsbad, CA) that contained 10% fetal bovine serum (JRH Biosciences, Lenexa, KS). After 3 hours (0 hours), unattached hepatocytes were washed out, and dimethyl sulfoxide (vehicle) or CCl_4 dissolved in dimethyl sulfoxide was added to the culture medium at a final concentration of 2.0 mmol/L. Then, total RNA was extracted from hepatocytes at 0, 3, 6, and 24 hours after CCl_4 administration. Isolated primary SECs were seeded in dishes coated with collagen type I-C (Nitta gelatin, Osaka, Japan) with Dulbecco's modified Eagle's medium/Ham's nutrient mixture F-12 (Sigma-Aldrich). After 12 hours, recombinant mouse Sema3e (R&D Systems) was added to the culture medium for a final concentration of 500 ng/mL. After incubation for 30 minutes, the morphologic status of SECs was analyzed by immunocytochemistry using fluorescein-conjugated phalloidin and Hoechst stain.

Forced Expression of Sema3e in Hepatocytes

We used the pLIVE vector and TransIT-EE Hydrodynamic Delivery solution (Mirus Bio, Madison, WI) to introduce Sema3e cDNA into 8-week-old mice by hydrodynamic tail-vein injection (HTVi). The primer pairs used for the expression vector are listed in Table 2.

Quantitative Analysis of Liver Sections Stained with Immunohistochemistry and Sirius Red

The vascular density was determined by analyzing stabilin (Stab)-2–positive area in the fields, including the central vein (CV). Four independent images of liver sections at ×200 magnification per animal were analyzed using the ImageJ software version 1.46r (NIH, Bethesda, MD). The parenchymal area was evaluated by subtracting vascular luminal area from the total field area and used for calculation. The fibrosis area was assessed by analyzing the Sirius Red–stained collagen areas in the liver sections at ×50 magnification. Ki-67–positive hepatocytes were counted using In Cell Analyzer 2000 (GE Healthcare), as described previously.[22]

Measurement of Serum ALT, Serum Albumin, and Hydroxyproline Content

Serum alanine aminotransferase (ALT) and albumin were measured at the Oriental Yeast Company (Tokyo, Japan) or by the Transaminase CII-test Wako (Wako). Hydroxyproline content was measured as described previously.[23]

Statistical Analysis

Statistical analysis was performed using the unpaired two-tailed Student's *t*-test. Gene expression in multiple liver cell fractions was compared by one-way analysis of variance and subsequent Tukey's tests. $P < 0.05$ was considered statistically significant.

Results

Sinusoidal Regeneration in CCl_4-Induced Liver Injury in Mice

The i.p. injection of CCl_4 produces a conventional liver injury model to study liver regeneration and subsequent fibrosis. We treated mice with CCl_4 and monitored the status of hepatocytes and SECs to investigate sinusoidal regeneration after liver injury. We have reported previously that Stab-2, a scavenger receptor, and receptors II (CD32) and III (CD16) for Fc fragment of IgG (FcγRs) are highly expressed in SECs and make it possible to distinguish SECs from other kinds of endothelial cells.[20,24] Frozen liver sections were subjected to immunohistochemistry (IHC) using

anti—Stab-2 or anti-FcγR antibodies, followed by H&E staining to visualize SECs in CCl_4-treated liver. Sinusoids in normal liver (0 hours) extended from the CV in a high-density radial pattern (Figure 1, A and B, and Supplemental Figure S1, A and B). Because CCl_4 is metabolized by cytochrome P450 in hepatocytes surrounding the CV to produce toxic free radicals as intermediate metabolites,[25] administering CCl_4 causes massive hepatocytic death around the CV. H&E staining revealed mild and obvious degeneration of hepatocytes at 24 and 48 hours after CCl_4 treatment, respectively (Figure 1, C and E, and Supplemental Figure S1, C and E). The sinusoidal structure was disorganized 24 hours after CCl_4 treatment, and most SECs in the degenerated region (Figure 1) seemed to be contracted, suggesting that some substantial alterations occurred in the SECs (Figure 1, C and D, and Supplemental Figure S1, C and D). The degenerated region became more obvious, and the arrangement of SECs remained disorganized 48 hours after CCl_4 treatment (Figure 1, E and F, and Supplemental Figure S1, E and F). Degeneration of hepatocytes decreased and hepatocytes regenerated 72 and 96 hours after CCl_4 treatment, but immune cells accumulated around the CV (Figure 1, G and I, and Supplemental Figure S1, G and I). In contrast, SECs returned to their original position and morphologic status during these phases (Figure 1, H and J, and Supplemental Figure S1, H and J). These data suggest that the process of sinusoidal regeneration would be completed by 72 hours after CCl_4-induced injury in mice.

Sema3e Is Expressed by Degenerating Hepatocytes during CCl_4-Induced Liver Injury

Because a sign of contraction was observed in SECs at 24 hours after CCl_4 treatment, it was supposed that some angiogenesis-related factors might be involved in this morphologic change. We found in our previous research about liver regeneration during chronic hepatitis that Sema3e is up-regulated in injured liver. Therefore, we examined the Sema3e expression pattern by quantitative RT-PCR (RT-qPCR) after CCl_4 treatment and measured serum concentrations of ALT as a liver injury marker (Figure 2, A and B). As a result, Sema3e expression was negligible in normal liver but was up-regulated drastically at 24 hours after CCl_4 treatment. Intriguingly, Sema3e expression then decreased sharply at 48 hours and returned to the basal level after 72 hours. These results suggest that up-regulation of Sema3e might be related with degeneration of hepatocytes, as evaluated by serum ALT (Figure 2, A and B), whereas rapid Sema3e down-regulation may represent completion of hepatocytic death. Therefore, we hypothesized that damaged hepatocytes could be a source for Sema3e. To address this hypothesis, we examined Sema3e expression in injured liver sections by IHC using an anti-Sema3e antibody. As expected, strong Sema3e signals were detected within the degenerating area around the CV 24 hours after CCl_4 treatment (Figure 2C). To investigate whether the cells expressing Sema3e were hepatocytes, we stimulated hepatocytes isolated from normal liver with CCl_4 in culture. Primary cultured hepatocytes became

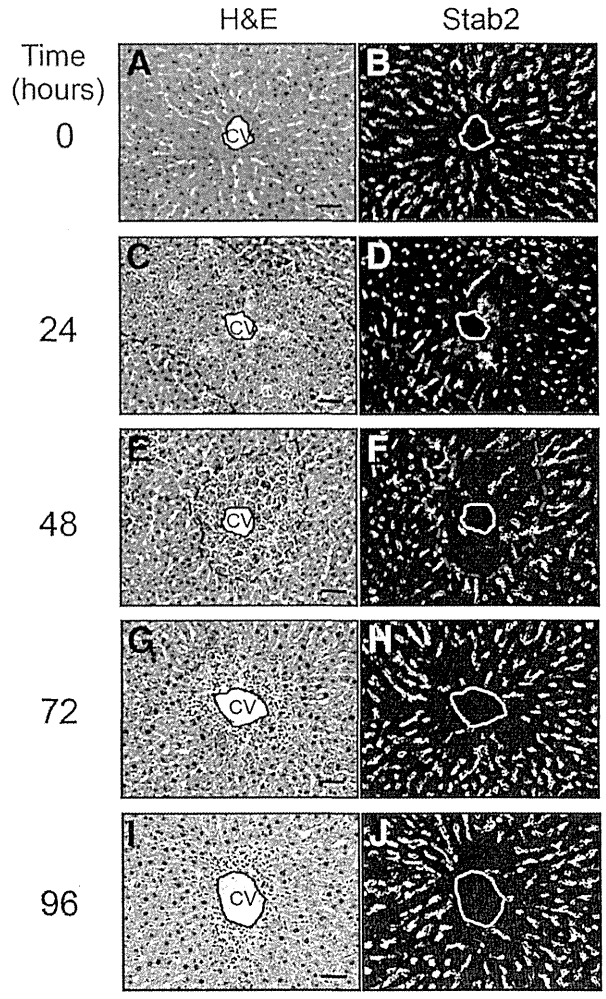

Figure 1 Morphologic transition of sinusoids after carbon tetrachloride (CCl_4)—induced liver injury. Identical sections were subjected to immunohistochemistry using anti-stabilin (Stab)-2 antibody and hematoxylin and eosin (H&E) staining (after immunostaining). **A** and **B:** The sinusoids extend from the central vein (CV) in a high-density radial pattern in normal liver (0 hours) before injury. **C** and **D:** Sinusoidal structure is affected 24 hours after CCl_4 treatment, followed by hepatocyte degeneration around the CV. **E** and **F:** Most sinusoidal endothelial cells (SECs) in the degenerated region (surrounded by the broken line) are strongly contracted. The arrangement of SECs remains disordered 48 hours after CCl_4 treatment. Degeneration of hepatocytes diminishes 72 (**G** and **H**) and 96 hours (**I** and **J**) after CCl_4 treatment, hepatocytes regenerate, and immune cells accumulate around the CV. Most of the SECs were stationed at the proper position during these phases. Scale bars: 50 μm (**A**, **C**, **E**, **G**, and **I**).

gradually swollen after CCl_4 treatment, and most of the hepatocytes degenerated 24 hours after CCl_4 challenge (Figure 2D). Real-time RT-PCR revealed that the expression level of Sema3e of CCl_4-treated hepatocytes was significantly increased compared with that of vehicle-treated or nontreated hepatocytes and 3.7-fold higher than that of injured liver 24 hours after *in vivo* administration of CCl_4 (whole liver), suggesting that damaged hepatocyte by oxidative stress is a major source of robust expression of Sema3e in CCl_4 injury model (Figure 2E). Although Sema3e is expressed in immune cells,[26] $CD45^+$ blood cells isolated from CCl_4-treated liver hardly expressed

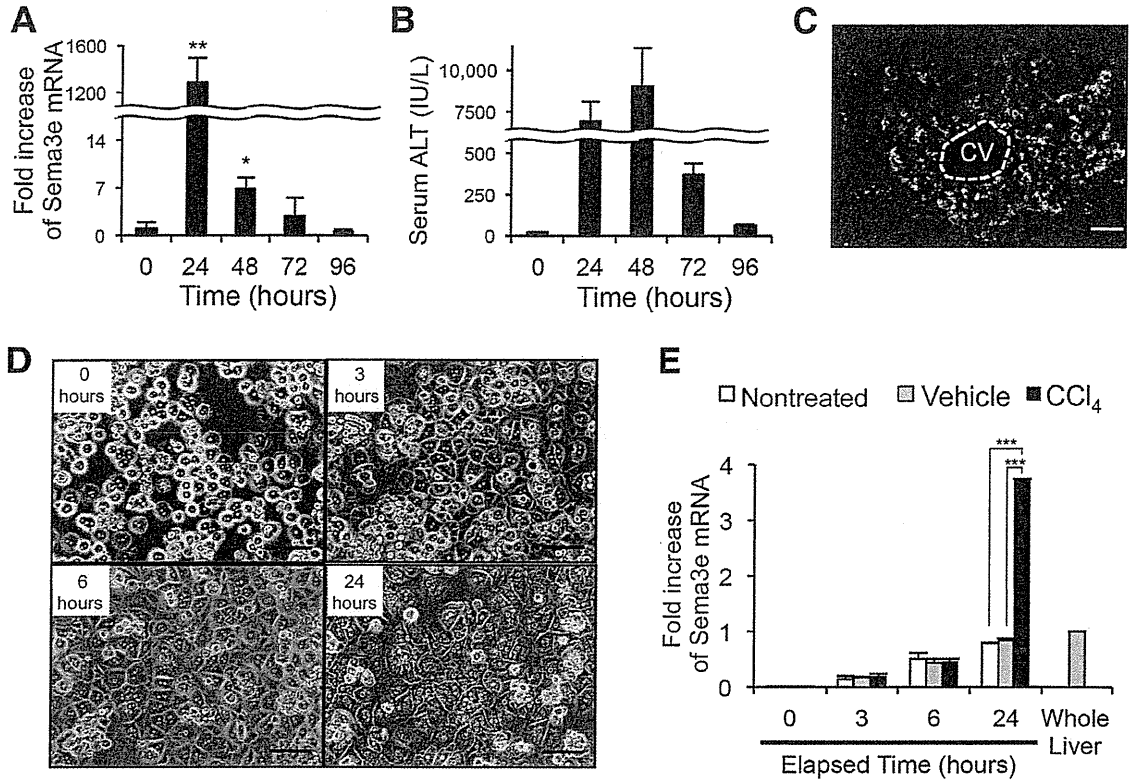

Figure 2 Expression profiles of semaphorin 3E (Sema3e) and plexin D1 (Plxnd1) in liver. **A:** Sema3e expression level in liver after carbon tetrachloride (CCl_4)—induced injury. **B:** Whole liver total RNA was assessed by quantitative RT-PCR. Evaluation of serum alanine aminotransferase level at indicated time points. **C:** Livers were subjected to immunohistochemical staining with an anti-Sema3e antibody 24 hours after CCl_4 treatment. Sema3e expression is observed in hepatocytes in the damaged region around the central vein. **D:** Morphologic alterations in primary cultured hepatocytes treated with CCl_4. **E:** The expression levels for *Sema3e* of primary cultured hepatocytes at 0, 3, 6, and 24 hours after nontreatment, vehicle treatment, or CCl_4 treatment, respectively. The whole liver represents the mRNA of injured mouse liver 24 hours after CCl_4 administration. The fold expression of Sema3e mRNA of cultured hepatocytes relative to the whole liver is shown. Data are expressed as means ± SEM. $n = 3$ per group. $^*P < 0.05$, $^{**}P < 0.01$, and $^{***}P < 0.001$ versus 0 hours after CCl_4 treatment. Scale bars: 50 μm (**C**); 100 μm (**D**).

Sema3e (Supplemental Figure S2A). Moreover, Sema3e was not induced after a 70% partial hepatectomy, which was not accompanied by hepatocyte damage (Supplemental Figure S2B). These results strongly suggest that Sema3e is induced in hepatocytes *in vitro* and *in vivo* in a damage-dependent manner.

Sema3e Has an Effect on Retracting SEC Filopodia

We isolated each type of liver cell by fluorescence-activated cell sorting and analyzed Sema3e receptor (Plxnd1) expression by RT-qPCR to identify the cell type that responded to Sema3e in injured liver. Plxnd1 was predominantly expressed in Stab-2^+ SECs (Figure 3A), suggesting that Sema3e secreted from degenerating hepatocytes could affect SECs in a paracrine fashion. Sema3e plays a role in repulsing the endothelial tip and inhibiting cell migration. However, the effect of Sema3e on SECs has not been examined. Therefore, we investigated the effect of Sema3e on freshly isolated SECs in culture. As a result, SEC filopodia retracted significantly in the presence of Sema3e (Figure 3, B and C), as reported previously in other endothelial cell lines.[18,27]

Prolonged Expression of Sema3e Results in Disoriented Sinusoidal Regeneration

Given that Sema3e also induced retraction of SEC filopodia *in vivo*, transient expression of Sema3e from damaged hepatocytes could be involved in the morphologic contraction of SECs as observed 24 hours after CCl_4 treatment (Figure 1D and Supplemental Figure S1D). This idea was supported by the result that SECs returned to their original morphologic status during reconstruction of sinusoids after the drastic decrease in Sema3e expression. To further verify Sema3e function *in vivo*, we examined the effect of prolonged Sema3e expression by HTVi, which is a method of delivering an expression vector into hepatocytes. We initially injected either Sema3e or a control expression vector into wild-type mice by HTVi. Then, each mouse was treated with either CCl_4 or vehicle 3 days after HTVi. We first examined SEC by using H&E and IHC staining 1 day after CCl_4 administration when endogenous Sema3e expression is drastically induced. We observed no obvious differences in the damaged area between control- and Sema3e-HTVi liver (Supplemental Figure S3). These results

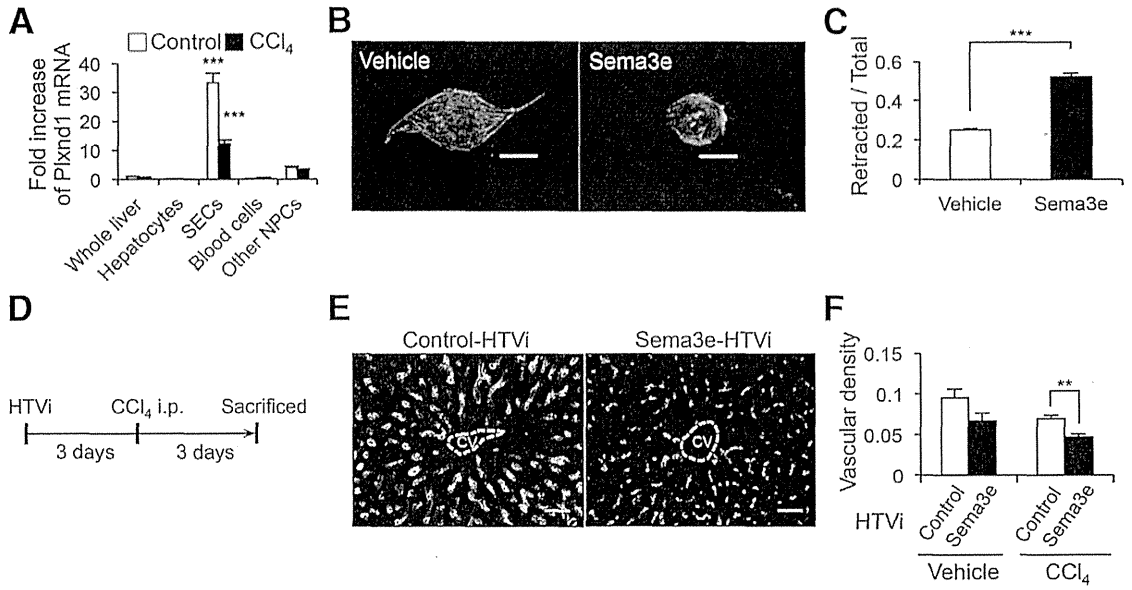

Figure 3 Semaphorin 3E (Sema3e) induces contraction of sinusoidal endothelial cells (SECs). **A:** Real-time RT-PCR analysis of plexin D1 (Plxnd1) in hepatocytes, SECs, blood cells, and other non-parenchymal cells (NPCs). Each fraction was isolated from normal or 24-hour post–carbon tetrachloride (CCl_4) liver, and Plxnd1 mRNA levels were compared with those of whole livers. Remarkable Plxnd1 expression was observed in SECs in normal and 24-hour post-CCl_4 livers. **B:** Morphologic changes in SECs after addition of Sema3e. **C:** SECs were subjected to primary culture with or without Sema3e. SECs cultured with Sema3e have significant retraction of filopodia observed in control SECs. **D:** Scheme of *in vivo* analysis using the hydrodynamic tail-vein injection (HTVi) method. **E:** The Sema3e expression vector was introduced into hepatocytes using the HTVi method. The mice were subjected to CCl_4 injection after 3 days. Then, livers were harvested after an additional 3 days. Immunostaining of liver sections with an anti–stabilin (Stab)-2 antibody 3 days after injury. **F:** Normal sinusoidal regeneration is observed in the control liver, whereas disorganized regeneration of contracted SECs is observed in Sema3e-expressed livers. Vascular density of control- and Sema3e-expressed liver sections before and after injury. The SEC area significantly decreases in Sema3e-expressed livers after liver injury. Vascular area was measured as Stab-2–positive area visualized by immunohistochemistry. Empty areas, such as the lumen, were subtracted for calculation. Data are expressed as means ± SEM. $n = 3$ per group (**A**); $n = 4$ per group (**C**); $n = 4$ to 5 per group (**F**). $^{**}P < 0.01$, $^{***}P < 0.001$ for analysis of variance with Tukey's post hoc tests. Scale bars: 20 μm (**D**); 50 μm (**F**).

suggested that the additional overexpression of Sema3e was not effective because the amount of endogenous Sema3e was enough to affect sinusoidal contraction 1 day after liver injury. Then, we analyzed the livers 3 days after CCl_4 administration when endogenous Sema3e expression is decreased (Figure 3D). Sinusoidal regeneration and SEC status were evaluated by IHC using an anti–Stab-2 antibody and vascular density, as represented by the ratio of the Stab-2–positive area to total parenchymal area (Figure 3, E and F). We confirmed that exogenous Sema3e expression by HTVi was maintained irrespective of CCl_4 treatment (Supplemental Figure S4). Although the vascular system of Sema3e-HTVi livers tended to decrease compared with that of control-HTVi livers, no significant difference was observed in vehicle treatment (Figure 3F). The Sema3e-HTVi liver treated with CCl_4 had markedly disoriented and contracted SECs, whereas radial arrays of SECs were reconstructed around the CV in control-HTVi liver (Figure 3E), which was similar to the image 24 hours after CCl_4 treatment (Figure 1D and Supplemental Figure S1D). Consistent with this observation, the vascular system of the Sema3e-HTVi liver decreased significantly compared with that of the control-HTVi liver (Figure 3F). These results suggest that Sema3e is able to affect the morphologic status of SECs in regeneration process *in vivo* and *in vitro*.

Disoriented Sinusoidal Regeneration by Sema3e Potentiates HSC Activation *in Vivo*

We examined whether regeneration of hepatocytes was affected after liver injury because inhibiting sinusoidal reconstruction in Sema3e-HTVi liver may affect blood flow in the liver. However, no significant differences were observed between control- and Sema3e-HTVi livers after H&E staining (Figure 4A) or by serum albumin concentration (Supplemental Figure S5). We next investigated the status of HSCs, another key component of the liver sinusoid. Because HSCs express p75 low-affinity neurotrophic growth factor receptor (p75NTR),[28,29] SECs and HSCs in a regenerating sinusoid were visualized by IHC using anti–Stab-2 and anti-p75NTR antibodies. Normal sinusoids were reconstructed in control-HTVi liver 3 days after CCl_4 treatment (ie, each HSC-lined SEC was rearranged correctly). In contrast, many extended HSCs were observed accompanied by disorganized revascularization in the Sema3e-HTVi liver (Figure 4B). Moreover, most of these HSCs were not lined by SECs. HSCs and SECs are reciprocally regulated, and transient activation of HSCs is beneficial for wound healing during regeneration. Therefore, we supposed that the activation of HSCs was prolonged because of the lack of regulation by SECs. Actually, an expression analysis of α-smooth

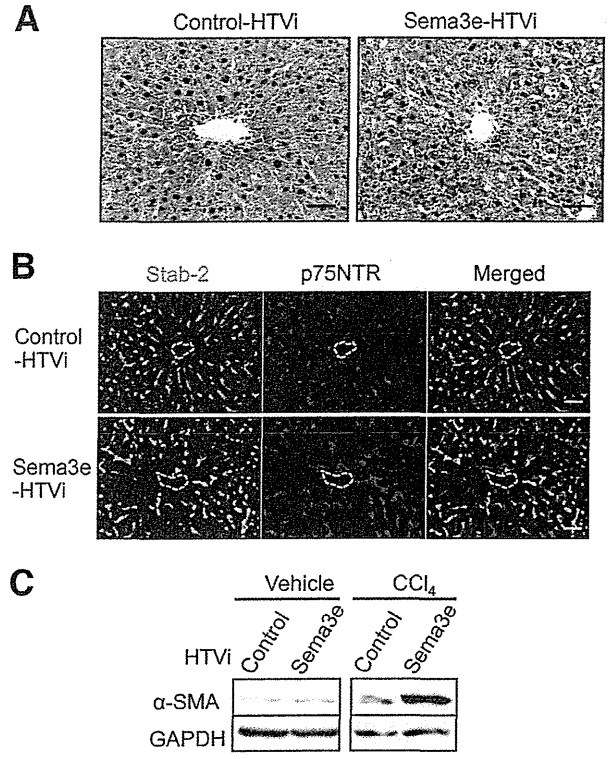

Figure 4 Disoriented sinusoidal regeneration by semaphorin 3E (Sema3e) potentiates hepatic stellate cell (HSC) activation *in vivo*. **A:** Hematoxylin and eosin staining of liver sections 3 days after carbon tetrachloride (CCl_4) treatment. No apparent difference is observed between control—hydrodynamic tail-vein injection (HTVi) and Sema3e-HTVi livers. **B:** Immunostaining of liver sections with anti—stabilin-2 (Stab-2) and anti-p75 low-affinity neurotrophic growth factor receptor (p75NTR) antibodies 3 days after CCl_4 treatment. Many HSCs in Sema3e-HTVi liver are not lined by sinusoidal endothelial cells (SECs) compared with that in control-HTVi liver. Broken line indicates central vein. **C:** Western blot analysis of α-smooth muscle actin (α-SMA) in liver 3 days after treatment with vehicle or CCl_4. α-SMA protein level in CCl_4-treated liver increases markedly in Sema3e-HTVi liver compared with the control, whereas the levels in vehicle-injected livers are not significantly different between Sema3e-HTVi and control-HTVi liver. Scale bar = 50 μm. GAPDH, glyceraldehyde-3-phosphate dehydrogenase.

muscle actin, an HSC activation marker, by Western blot analysis revealed activation of HSCs in Sema3e-HTVi liver compared with that in control-HTVi liver (Figure 4C). In contrast, the vehicle treatment did not activate the HSCs irrespective of continuous Sema3e expression, suggesting that Sema3e does not directly activate uninjured HSCs. Thus, Sema3e is likely to activate HSCs through SECs only when the sinusoid is undergoing reconstruction. These results suggest that transient expression of Sema3e by degenerating hepatocytes might contribute to the initial step of wound healing by activating HSCs.

Consecutive Expression of Sema3e Is a Risk Factor for Liver Fibrosis

Hepatocytes continue to be damaged in chronic hepatitis, and sinusoids are regenerated repeatedly. Given that continuous Sema3e expression resulted in activating HSCs, consecutive exposure of Sema3e under chronic hepatitis might contribute to the risk of fibrosis through prolonged HSC activation. We used *Sema3e*-KO mice to address this hypothesis. First, we compared hepatocellular damage induced by a single administration of CCl_4 between wild-type and *Sema3e*-KO mice. We found no significant difference in serum ALT level between both genotypes after CCl_4 administration (Supplemental Figure S6), suggesting that Sema3e deficiency does not directly affect the CCl_4-mediated hepatocellular cytotoxicity. Second, we evaluated the morphologic status of SECs and HSCs 24 hours after

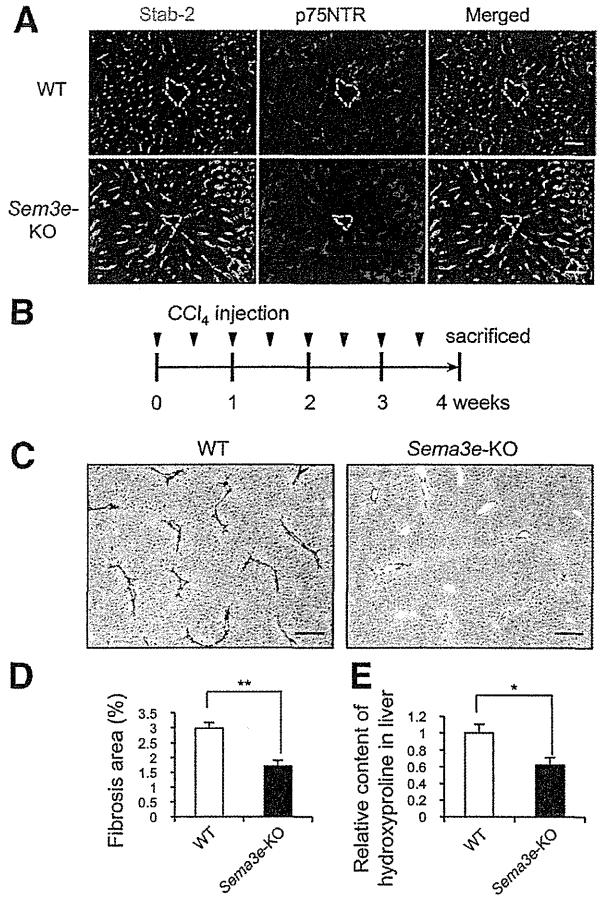

Figure 5 Lack of semaphorin 3E (Sema3e) affects sinusoidal regeneration and attenuates liver fibrosis. **A:** Immunostaining of liver sections with anti—stabilin-2 (Stab-2) and anti-p75 low-affinity neurotrophic growth factor receptor (p75NTR) antibodies 24 hours after carbon tetrachloride (CCl_4) treatment. **B:** Sinusoidal endothelial cell (SEC) morphologic status in wild-type (WT) mice is markedly contracted, whereas that of *Sema3e*-knockout (KO) mice is less affected. Broken line indicates central vein (CV). Experimental scheme for liver fibrogenesis in wild-type and *Sema3e*-KO mice. **C** and **D:** A total of 1.0 mL/kg of i.p. CCl_4 was injected into each mouse twice per week for 4 weeks, and then the liver was harvested. Sirius Red staining of liver sections after CCl_4 treatment. **E:** WT mouse liver exhibits marked accumulation of fibers around the CV, whereas the *Sema3e*-KO mouse liver appears less fibrotic. Relative hydroxyproline (Hp) content in liver. *Sema3e*-KO livers contain less Hp than WT livers. Data are expressed means ± SEM. $n = 5$ per group. $^*P < 0.05$, $^{**}P < 0.01$. Scale bars: 50 μm (**B**); 200 μm (**E**).

CCl_4 treatment in wild-type and *Sema3e*-KO mice. The SECs were markedly contracted in wild-type mice, whereas they were less affected in *Sema3e*-KO mice (Figure 5A). These results indicate that not only the robust expression of Sema3e but also the lack of Sema3e could affect sinusoidal regeneration. Moreover, almost all HSCs were associated with SECs in *Sema3e*-KO mice, but many HSCs were not lined by SECs in wild-type mice (Figure 5A). Finally, the morphologic features of both wild-type and *Sema3e*-KO SECs reverted to the original shape 72 hours after CCl_4 treatment (Supplemental Figure S7).

To further investigate the involvement of Sema3e in liver regeneration and fibrosis, chronic hepatitis was induced in wild-type and *Sema3e*-KO mice by repeated administration of CCl_4 (Figure 5B). We investigated the proliferation of hepatocytes 72 hours after the final CCl_4 injection by IHC using an anti–Ki-67 antibody. We found no significant differences in the rate of Ki-67–positive hepatocytes around the CV between wild-type and *Sema3e*-KO mice (Supplemental Figure S8, A and B). However, Picro Sirius Red staining revealed that the accumulation of collagen fibers was markedly decreased in *Sema3e*-KO mice compared with wild-type mice (Figure 5, C and D). Actually, the hydroxyproline content in liver, which reflects the amount of collagen, decreased significantly in *Sema3e*-KO mice compared with wild-type mice (Figure 5E), indicating that the lack of Sema3e attenuates liver fibrosis. In addition, *Sema3e*-KO SECs around the CV exhibited a more extended morphologic status than wild-type SECs even after chronic injury (Supplemental Figure S9). These results indicate that continuous exposure to Sema3e under a chronic hepatitis condition contributes to the exacerbation of liver fibrosis.

Discussion

We found that Sema3e plays significant roles in sinusoidal regeneration and the progression of liver fibrosis (Figure 6). We found that damaged hepatocytes transiently expressed Sema3e, which induced contraction of SECs in CCl_4-mediated liver injury model. Because free radical derived from CCl_4 metabolite damages the liver cells, we cannot exclude the possibility that cytotoxicity or cellular alterations due to proteolysis may partly contribute to the thinner staining of SECs by IHC. However, the staining patterns by two distinct SEC surface markers, Stab-2 and FcγR, exhibited a similar contracted morphologic status. In addition, *Sema3e*-KO SECs were less contracted than wild-type SECs after CCl_4 administration despite no significant differences in hepatocellular cytotoxicity, strongly suggesting that contraction of SEC was caused by Sema3e actively rather than passive cellular alterations.

Various functions of semaphorins and their receptors have been revealed recently. Among them, regulation of angiogenesis as a repulsive cue is a well-known function of type 3 semaphorins. In particular, Sema3e inhibits extension of endothelial tip cells that play a significant role in angiogenic guidance. In contrast, Sema3e and Plxnd1 are expressed in macrophages of advanced atherosclerotic plaques and regulate their retention.[26] However, the functional significance of Sema3e in liver disease remains unknown. Because Sema3e and Plxnd1 mRNA were not detected in CD45-positive blood cells, including macrophages in either normal or CCl_4-treated liver, it is unlikely that blood cells are related to a series of SEC morphologic changes directly. Meanwhile, Sema3e expression was induced in damaged hepatocytes. Although the signaling pathway implicated in Sema3e expression is largely unknown, Moriya et al[30] found that p53 expression up-regulated Sema3e expression in HUVEC and ischemic limb. Considering that reactive oxygen species (ROS) relate to the activation of p53 signaling,[31] drastic expression of Sema3e in CCl_4-injured liver may be promoted in a p53-dependent manner. In addition, the modest induction of Sema3e in primary cultured hepatocytes without ROS suggests the possibility that a cellular stress by dissociation or culture is involved in Sema3e expression. In fact, we have observed that the other hepatitis models, such as concanavalin-A injection or 3,5-diethoxycarbonyl-1,4-dihydrocollidine feeding, also induce potent expression of Sema3e (data not shown), suggesting the existence of another pathway independent of ROS stimuli. Further studies are needed to elucidate alternative signaling pathways.

Secreted type 3 semaphorins have been considered to function in an autocrine manner during angiogenesis. However, our findings indicate that Sema3e may play a

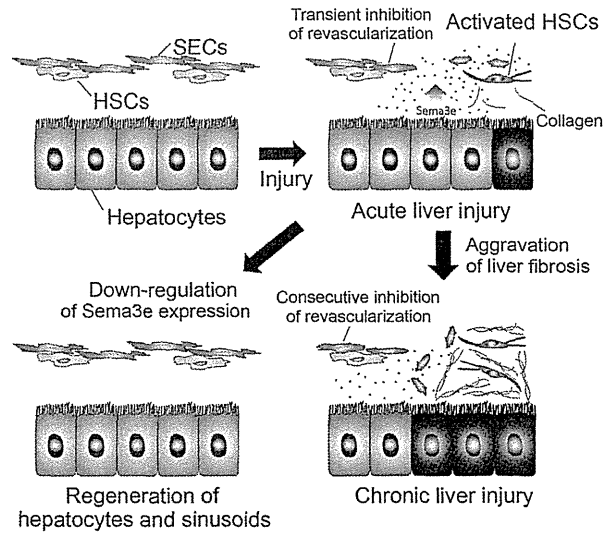

Figure 6 A model of the regulatory mechanism of sinusoidal regeneration and liver fibrosis by semaphorin 3E (Sema3e) signaling. Damaged hepatocytes express Sema3e transiently to promote contraction of sinusoidal endothelial cells (SECs), which diminishes the influence by hepatic stellate cells (HSCs). Consequently, isolated HSCs are more easily activated to promote liver regeneration during wound healing. However, consecutive Sema3e expression during chronic liver injury causes sustained inhibition of sinusoidal regeneration and HSC activation, resulting in collagen accumulation.

significant role not only in the regulation of sinusoidal regeneration but also in fibrogenesis through HSCs in a paracrine manner. The Sema3e/Plxnd1 axis counteracts VEGF/VEGFR-2 signaling via a feedback mechanism.[19] Because selective activation of VEGFR-1 on SECs stimulates hepatocyte proliferation *in vivo* and reduces liver damage in mice exposed to CCl_4,[32] transient expression of Sema3e may contribute to liver regeneration by skewing VEGFR-2 signaling to VEGFR-1. Alternatively, considering that the activation of SECs and/or HSCs contributes to the proliferation of hepatocytes by producing mitogenic cytokines, the regeneration of hepatocytes may be aberrant in *Sema3e*-KO mice. Although no significant difference was found in hepatocyte proliferation between wild-type and *Sema3e*-KO mice after chronic liver injury, further investigation will be required to make a conclusion.

In terms of physiologic significance of transient Sema3e expression by damaged hepatocytes, its possible role in wound repair will be taken into account. The recruitment of immune cells to a damaged site is a step for wound healing.[33] Macrophages operate as voracious phagocytes, clearing the wound of all matrix and cell debris. Therefore, enhanced permeability and decreased density of sinusoids by Sema3e could contribute to wound repair by facilitating the migration of immune cells to damaged region.

Because a massive volume of blood flows into the liver sinusoids, a fine balance between proangiogenic and antiangiogenic signaling is required for liver homeostasis. For example, VEGF, the primary proangiogenic factor in sinusoidal regeneration, is transiently up-regulated after liver injury.[34] However, constitutive expression of VEGF, which is induced by chronic liver injury, results in aberrant angiogenesis and the development of abnormal vascular architecture that is strongly linked to progressive fibrogenesis.[35] Thus, disrupting the balance leads directly to pathologic changes. Therefore, transient expression of Sema3e by damaged hepatocytes may contribute to the fine-tuning of sinusoidal regeneration and the inhibition of aberrant angiogenesis. Taken together, our results suggest that Sema3e contributes to the initial steps of liver regeneration by providing a scaffold for proliferating hepatocytes through activating HSCs. In addition, progressive fibrogenesis could be caused not only by consecutive expression of a proangiogenic factor but also by an antiangiogenic factor. In conclusion, our findings indicate that Sema3e is the main antiangiogenic player of SECs during liver injury and that consecutive Sema3e expression is a risk factor for liver fibrosis. These results suggest that Sema3e or Plxnd1 could be a therapeutic target in liver fibrosis and cirrhosis.

Acknowledgments

We thank Dr. Yutaka Yoshida and Dr. Atsushi Kumanogoh for providing *Sema3e*-KO mice, Naoko Miyata for assistance with flow cytometry, Yoshiko Kamiya for mouse and technical assistance, and the members of the Miyajima laboratory for helpful discussion and suggestions.

Supplemental Data

Supplemental material for this article can be found at *http://dx.doi.org/10.1016/j.ajpath.2014.04.018*.

References

1. Taub R: Liver regeneration: from myth to mechanism. Nat Rev Mol Cell Biol 2004, 5:836–847
2. Selden AC, Hodgson HJ: Growth factors and the liver. Gut 1991, 32: 601–603
3. Michalopoulos GK, DeFrances MC: Liver regeneration. Science 1997, 276:60–66
4. Raghow R: The role of extracellular matrix in postinflammatory wound healing and fibrosis. FASEB J 1994, 8:823–831
5. Zhang DY, Friedman SL: Fibrosis-dependent mechanisms of hepatocarcinogenesis. Hepatology 2012, 56:769–775
6. Friedman SL, Roll FJ, Boyles J, Bissell DM: Hepatic lipocytes: the principal collagen-producing cells of normal rat liver. Proc Natl Acad Sci U S A 1985, 82:8681–8685
7. DeLeve LD, Wang X, Hu L, McCuskey MK, McCuskey RS: Rat liver sinusoidal endothelial cell phenotype is maintained by paracrine and autocrine regulation. Am J Physiol Gastrointest Liver Physiol 2004, 287:G757–G763
8. Deleve LD, Wang X, Guo Y: Sinusoidal endothelial cells prevent rat stellate cell activation and promote reversion to quiescence. Hepatology 2008, 48:920–930
9. Tanaka H, Leung PS, Kenny TP, Gershwin ME, Bowlus CL: Immunological orchestration of liver fibrosis. Clin Rev Allergy Immunol 2012, 43:220–229
10. Nishina T, Komazawa-Sakon S, Yanaka S, Piao X, Zheng DM, Piao JH, Kojima Y, Yamashina S, Sano E, Putoczki T, Doi T, Ueno T, Ezaki J, Ushio H, Ernst M, Tsumoto K, Okumura K, Nakano H: Interleukin-11 links oxidative stress and compensatory proliferation. Sci Signal 2012, 5:ra5
11. Li F, Huang Q, Chen J, Peng Y, Roop DR, Bedford JS, Li CY: Apoptotic cells activate the "phoenix rising" pathway to promote wound healing and tissue regeneration. Sci Signal 2010, 3:ra13
12. Okabe M, Tsukahara Y, Tanaka M, Suzuki K, Saito S, Kamiya Y, Tsujimura T, Nakamura K, Miyajima A: Potential hepatic stem cells reside in EpCAM+ cells of normal and injured mouse liver. Development 2009, 136:1951–1960
13. Inagaki FF, Tanaka M, Inagaki NF, Yagai T, Sato Y, Sekiguchi K, Oyaizu N, Kokudo N, Miyajima A: Nephronectin is upregulated in acute and chronic hepatitis and aggravates liver injury by recruiting CD4 positive cells. Biochem Biophys Res Commun 2013, 430: 751–756
14. Yazdani U, Terman JR: The semaphorins. Genome Biol 2006, 7:211
15. Zhou Y, Gunput RA, Pasterkamp RJ: Semaphorin signaling: progress made and promises ahead. Trends Biochem Sci 2008, 33:161–170
16. Gu C, Giraudo E: The role of semaphorins and their receptors in vascular development and cancer. Exp Cell Res 2013, 319:1306–1316
17. Gu C, Yoshida Y, Livet J, Reimert DV, Mann F, Merte J, Henderson CE, Jessell TM, Kolodkin AL, Ginty DD: Semaphorin 3E and plexin-D1 control vascular pattern independently of neuropilins. Science 2005, 307:265–268
18. Sakurai A, Gavard J, Annas-Linhares Y, Basile JR, Amornphimoltham P, Palmby TR, Yagi H, Zhang F, Randazzo PA, Li X, Weigert R, Gutkind JS: Semaphorin 3E initiates antiangiogenic signaling through plexin D1 by regulating Arf6 and R-Ras. Mol Cell Biol 2010, 30:3086–3098